Experimental Staphylococcus aureus brain abscess.

D R Enzmann, R R Britt, W G Obana, J Stuart and K Murphy-Irwin

AJNR Am J Neuroradiol 1986, 7 (3) 395-402
http://www.ajnr.org/content/7/3/395

Experimental *Staphylococcus Aureus* Brain Abscess

Dieter R. Enzmann[1]
Richard R. Britt[2]
William G. Obana[3]
Jeff Stuart[4]
Kathleen Murphy-Irwin[1]

The virulent organism *Staphylococcus aureus* produced brain abscesses that were quantitatively and qualitatively different from those caused by less virulent organisms. *S. aureus* abscesses created larger lesions, as earlier ependymitis, delayed progress toward healing, and caused areas of inflammatory escape outside the collagen capsule. Imaging tests revealed similar findings: the abscesses were larger, had more extensive central necrosis, and showed earlier evidence of ependymitis. This virulent organism also demonstrated that white matter is more susceptible than overlying gray matter to destruction by infection. The pattern of spread and other histologic findings suggest that collagen capsule formation has less of an infection "containment" function than was previously thought.

Several different types of bacterial organisms have now been studied in different experimental brain abscess models [1–6, 8, 10, 11–21]. The stages of the bacterial infection as it progresses to a well-formed brain abscess have been characterized neuropathologically and correlated with imaging techniques, such as X-ray computed tomography (CT) and high-resolution ultrasound (US) [1–11, 20, 21]. Although the major neuropathologic stages are relatively stereotyped, the rate at which infection progresses through these stages differs for various organisms, as demonstrated by our study of alpha streptococcus and a mixed infection of *Bacteroides fragilis* and *Staphylococcus epidermidis* [1–6, 10]. An experimental canine brain abscess was produced by *Staphylococcus aureus* to investigate the neuropathologic, CT, and US correlations of a more virulent bacterial organism.

Materials and Methods

Abscess Induction

Brain abscess was induced in 13 dogs by a direct-inoculation technique. The organism used to produce the abscess was *Staphylococcus aureus.* An inoculum of this organism was mixed with an equal volume of 1% agarose and drawn into a 1-ml syringe: 0.3 to 0.8 ml of this mixture was injected 5 mm deep into the parietal white matter, delivering approximately 108 colony-forming units (CFU). The rest of the surgical procedure was as previously described [1–6].

CT Scans

CT scanning was performed in the coronal projection on the Varian CT and G. E. CT (8800) scanners. Both scanners utilized 10-mm contiguous slice thickness. A bolus of 60% diatrizoate meglumine (4 ml/kg) was injected intravenously and followed immediately by a CT scan defined as the "zero minute" scan. Sequential scans through the center of the abscess were then performed at 5, 10, 20, 30, 45, and 60 min. Serial CT studies were performed at 3- to 5-day intervals until the dogs were killed.

Contrast enhancement was evaluated by defining a region of interest (4 to 8 pixels) in the ring (a representative area on the cortical side) or nodular area of enhancement. A baseline

Received April 24, 1985; accepted after revision August 29, 1985.

This work was supported by NIH Grant NS-16404-03.

[1] Department of Radiology, Division of Diagnostic Radiology, Stanford University Medical Center, Stanford, CA 94305. Address reprint requests to D. R. Enzmann.

[2] Department of Surgery, Division of Neurosurgery, Stanford University Medical Center, Stanford, CA 94305.

[3] University of California Medical School, San Francisco, San Francisco, CA 94143.

[4] Stanford University, Stanford, CA 94305.

***AJNR* 7:395–402, May/June 1986**
0195–6108/86/0703–0395

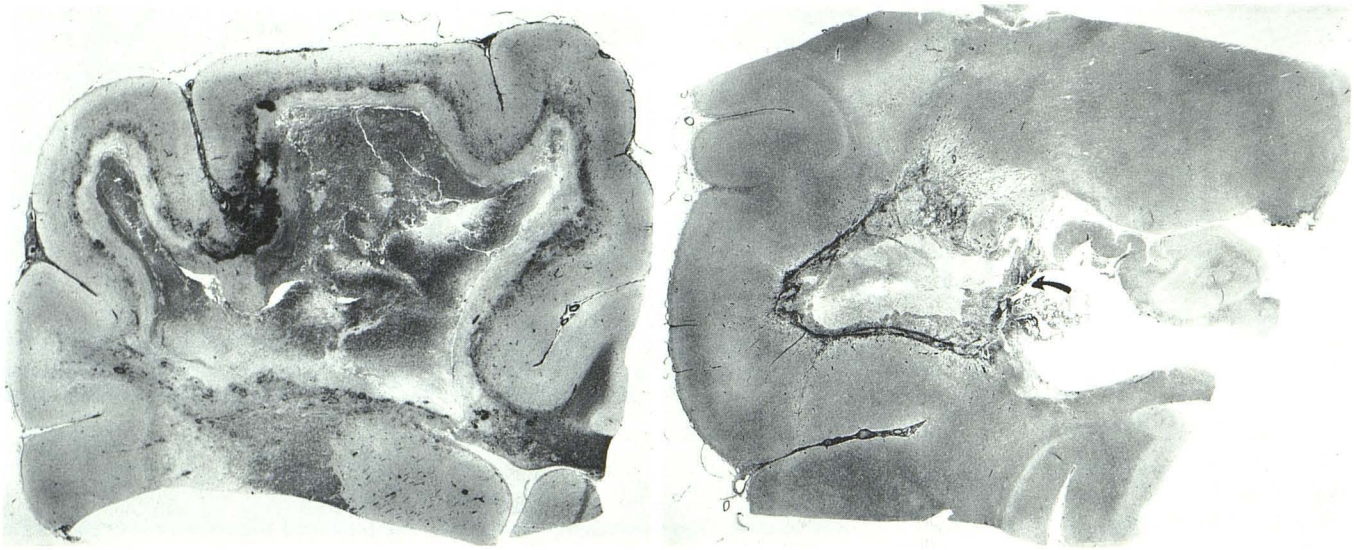

A B

Fig. 1.—Gross pathologic sections of a staphylococcal abscess 5 days (**A**) and 21 days (**B**) after inoculation. The early cerebritis stage is characterized by extensive inflammatory necrosis of the cerebral white matter and distinctive sparing of the overlying ribbon of cortical gray matter. The numerous black punctate and sometimes more confluent areas at the gray–white junction represent perivascular hemorrhages. The infection appeared to cause vessel thrombosis and hemorrhage as the cerebral vessels penetrated into the white matter (reticulin stain, ×5). The corresponding CT is seen in Figure 4. In the capsule stage, the abscess is still restricted to deep white matter (**B**). The collagen capsule (dark stain) is well formed on the cortical site of the abscess but less well developed on the ventricular side. Ventricular rupture had occurred where the capsule was poorly developed (*arrow*).

attenuation value for the normal brain was obtained in an analogous area in the contralateral hemisphere. Contrast enhancement was expressed in units above this baseline.

Ultrasound Scans

US scans, performed at the same time as CT scans, produced coronal and sagittal views through the abscess by means of a 5- and 7.5-MHz sector scanner (Diasonics). The transducer was small, with a face diameter of 16 mm, allowing full access to the brain through the craniotomy site. Images were recorded on film with a multiformat camera.

Neuropathology

Neuropathologic evaluation was accomplished by killing the animals at the following time intervals after inoculation: days 3, 4 (two dogs), 5 (two dogs), 7, 9, 11, 12, 14, 15, 18, and 21. In each case, the dog's entire brain was removed and immediately placed in 10% formalin for a period of at least 5 weeks. The brain was then cut into 0.5-cm coronal sections and photographed for comparison with US and CT scans. An area encompassing the entire abscess was then cut for further processing. General cytologic features were assessed by using hematoxylin and eosin; the presence of bacteria was assessed by gram stain; and reticulin or precollagen production was assessed with the reticulin stain. Masson trichrome and hematoxylin van Giesen stains were used to determine the presence of mature collagen, and phosphotungistic acid and glial fibrillary acid protein stains were used to evaluate reactive astrocytosis.

Results

Abscess formation was classified into four main stages: early cerebritis, late cerebritis, early capsule formation, and late capsule formation. The time sequence of neuropathologic changes was described in our alpha streptococcus model, modified somewhat for use with *B. fragilis*, and now modified even further for the *Staphylococcus aureus* brain abscess. The modification primarily entailed extending the time interval for each stage, since the entire process toward resolution took longer than it did with alpha streptococcus and even somewhat longer than with *B. fragilis*. The early cerebritis stage spanned days 1 through 5 after inoculation; the late cerebritis stage, days 6 through 11; the early capsule stage, days 12 through 18; and the late capsule stage, day 19 and beyond.

Early Cerebritis Stage (Days 1–5)

This early stage was characterized by extensive and widespread inflammatory necrosis, which, however, was sharply limited to white matter (Fig. 1). This necrosis was demarcated at the gray–white junction. The central portion of the infection showed coagulative necrosis, whereas the peripheral zone showed an extensive acute inflammatory infiltrate composed of polymorphonuclear leukocytes, lymphocytes, and plasma cells. Scattered within this inflammatory zone were large areas of protein-rich fluid. Outside the dense, acute inflammatory infiltrate in both gray and white matter were scattered areas of cerebritis characterized by perivascular, inflammatory infiltrates. In other areas, however, the necrosis and dense, acute inflammatory infiltrate was sharply demarcated from adjacent brain parenchyma. This latter finding suggested rapid extension, since the adjacent brain had not shown a "cerebritis" type response. In the areas lacking cerebritis there was an extensive exudate of proteinaceous fluid and edema.

Another indication of the rapid spread of infection was the early detection (by day 3) of ependymal rupture, ependymitis, and choroiditis (Fig. 2). A prominent finding at the end of the cerebritis stage was the thrombosis of small and large vessels and prominent ringlike perivascular hemorrhages (Fig. 3). These were seen primarily at the periphery of the infection and in parenchyma outside the acute inflammatory infiltrate. At the end of this stage, a small amount of perivascular reticulin, but no collagen, was detected. As a harbinger of things to come, some of the vessels that had begun to sprout reticulin were already isolated within the necrotic center and inside the advancing edge of the infection. This was another sign of rapid spread and difficulty in containment.

The CT scan findings in the early cerebritis stage were consistent with the neuropathologic findings in that each dog showed a large, low-density lesion in the parietal lobe, often extending from the cortical surface to the ventricle. Adjacent vasogenic edema with its fingerlike projections was prominent. The mass effect causing a midline shift was marked even at this early stage. On day 3, contrast enhancement was faint and often only partial at the lesion's edge despite its large size (Fig. 4). As early as day 3, however, the CT scan showed evidence of ventricular rupture as evidenced by increased contrast enhancement of the choroid plexus (Fig. 4). At the end of the early cerebritis stage (day 5), contrast enhancement became more prominent and was seen as a complete ring around the large, low-density lesions (Fig. 5). At this time, delayed scans showed some diffusion of the contrast into the low-density center, resulting in a thickened ring. None of the abscesses, however, completely filled in the lesion. The US scan showed large, hypoechoic lesions, representing the area of inflammatory necrosis, and a thin rim of hyperechogenicity at the periphery, representing the inflammatory infiltrate (see Fig. 8A).

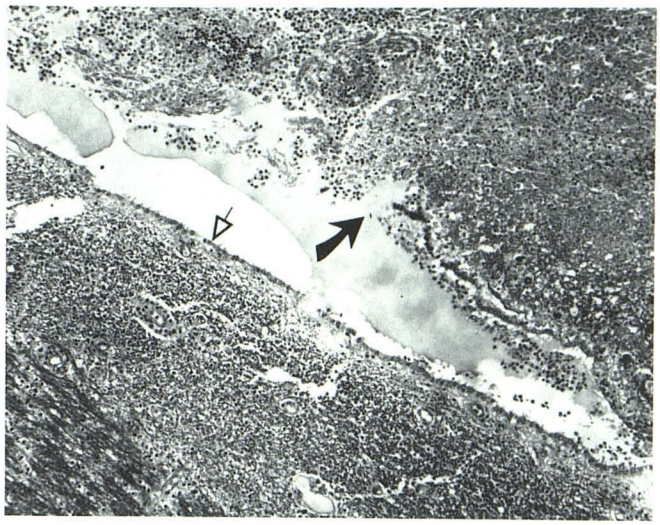

Fig. 2.—This photomicrograph shows rupture of the inflammatory process through the ependyma (*closed arrow*) with spillage of proteinaceous fluid into the ventricle. The ependyma (*open arrow*) is seen as a single lining of cuboidal epithelium (trichrome, ×125).

Fig. 3.—Numerous perivascular hemorrhages occurred around thrombosed vessels at the edge of the infection and especially at the junction of the gray and white matter. These were seen early, as in this day-5 staphylococcal abscess (trichrome, ×200).

Late Cerebritis Stage (Days 6–11)

At this stage, the large area of necrosis and the character of the inflammatory infiltrate were unchanged. The necrosis still was limited primarily to white matter. Although cerebritis (acute perivascular infiltrates) was more prominent in both gray and white matter, there still remained areas of advancing infection where the adjacent parenchyma did not exhibit cerebritis. At this time, the typical abscess zones of necrotic center, the inflammatory infiltrate mixed with macrophages lining the necrotic center, the area of reticulin and collagen formation, the peripheral areas of cerebritis, and the surrounding cerebral edema were better demarcated than in the previous stage. Perivascular reticulin formation and mature collagen development became evident during this stage. Both reticulin and collagen formation were greater on the cortical side, in the gray matter, than on the ventricular side, which was primarily in the white matter. There were areas of advancing infection in which virtually no reticulin or collagen reaction could be detected. It was at this stage that "escape" became evident, a phenomenon characterized histologically by extension of the infection—with its inflammatory and edematous changes—beyond an area in which significant reticulin and collagen formation had already taken place. The reticulin became fragmented and partially destroyed, and it was now located within the large area of necrosis (Fig. 6C). A futile attempt was made to wall off the infection. Reactive astrocytosis was minimal.

The CT scan continued to show a large, low-density lesion that was larger than it was at the early cerebritis stage. These areas were now consistently ringed by an area of contrast enhancement, but there was diffusion of the contrast material toward the necrotic center on delayed scans. This decrease in diffusion correlated with central necrosis and the lack of vascularity. During this stage the lesions reached their largest size, ring enhancement was at its greatest diameter, and

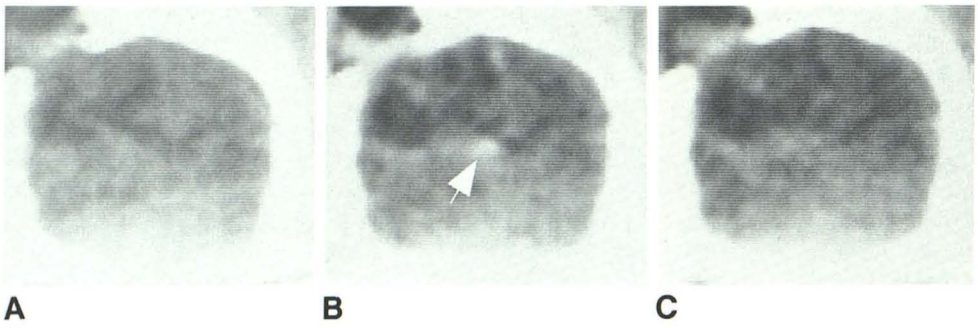

Fig. 4.—Serial CT scans (**A**, precontrast; **B**, 10 min postinfusion; **C**, 60 min postinfusion) of a staphylococcal abscess 3 days after inoculation. The area of cerebritis is seen as a large, low-density lesion with faint peripheral contrast enhancement that does not form a complete ring. Note the already prominent asymmetrical enhancement of the ipsilateral choroid plexus (**B**, *arrow*). This latter finding indicated early ventriculitis.

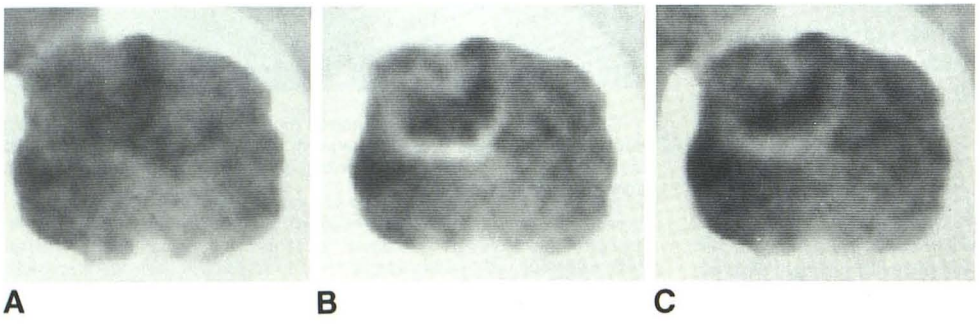

Fig. 5.—Serial CT scans (**A**, precontrast; **B**, 10 min postinfusion; **C**, 60 min postinfusion) of a staphylococcal abscess 5 days after inoculation. The CT scan corresponds closely to the pathological specimen shown in Fig. 1. The lesion is seen as a large, low-density area with peripheral contrast enhancement forming a complete ring. Note the scalloped outer border conforming to the white matter–gray matter border, seen pathologically. Some thickening of the ring is seen on the delayed scan (**C**), but a large portion of the central area does not show diffusion, indicating complete necrosis. Displacement of the ventricular system suggests the marked mass effect.

vasogenic edema and mass effect were at their maximum. Evidence for ventriculitis at this stage was reflected by an abnormally increased enhancement of the choroid plexus and by ventricular dilation in the face of severe mass effect. Ventricular dilation was often noted on the contralateral side, whereas the ipsilateral side was compressed by the large lesion. The US scan showed changes similar to the CT scan in that the lesion, both in the area of the hypoechoic center and in the hyperechoic ring, increased in size. The ependymitis appeared as increased echogenicity of the choroid plexus within the ventricle.

Early Capsule Stage (Days 12–18)

At this stage, the infection was better contained than in the previous stage, and there was good capsule development on the cortical side, as evidenced by marked reticulin and collagen formation. On the ventricular side of the infection, however, capsule formation was still poor with only moderate reticulin and minimally mature collagen deposition. The phenomenon of "escape" was again seen, with areas of necrosis, edema, and protein-rich fluid extending beyond what appeared to be a relatively well formed capsule. The reticulin did not appear to be as fragmented as it was in the previous stage, but there was little doubt that the integrity of the capsule had been violated. This phenomenon of "escape" occurred even in abscesses that had relatively good capsule formation, but it was never seen on the cortical side of the abscess. At no time did necrosis penetrate the gray matter. Ependymitis, when present, was well developed with a marked inflammatory response within the ventricle and choroid plexus. Collagen production was abundant in the choroid plexus. Gram stains were positive throughout the early and late cerebritis stages, but organisms could no longer be detected in the early capsule stage.

The CT scan during this stage showed a lesion of decreased size both in the area of low density and in the diameter of ring-contrast enhancement (Fig. 7). Ring enhancement was complete and did not show significant inward diffusion on delayed CT scans. Although the lesion had decreased in size, the amount and extent of surrounding vasogenic edema remained unchanged and near its maximum. At this time, the CT scan showed more extensive ependymitis, as indicated by enhancement of a greater portion of the of the ventricular system, and it often showed large areas of solid enhancement that filled the entire lateral ventricle or the temporal horn (see Fig. 9). At this stage, the ventricular system was consistently dilated as compared with earlier stages (Fig. 7). The US scan showed similar decreases in the size of the hypoechoic center and the hyperechoic ring (Fig. 8).

Late Capsule Stage (Day 19 and on)

At this stage, reticulin and mature collagen formation around the area of inflammation had progressed to form a solid capsule. Compared with the previous stage, the necrotic center had decreased in size and the inflammatory infiltrate had changed in character. The foamy macrophages that had appeared in the early capsule stage were greatly increased in number and now dominated the inflammatory infiltrate. They

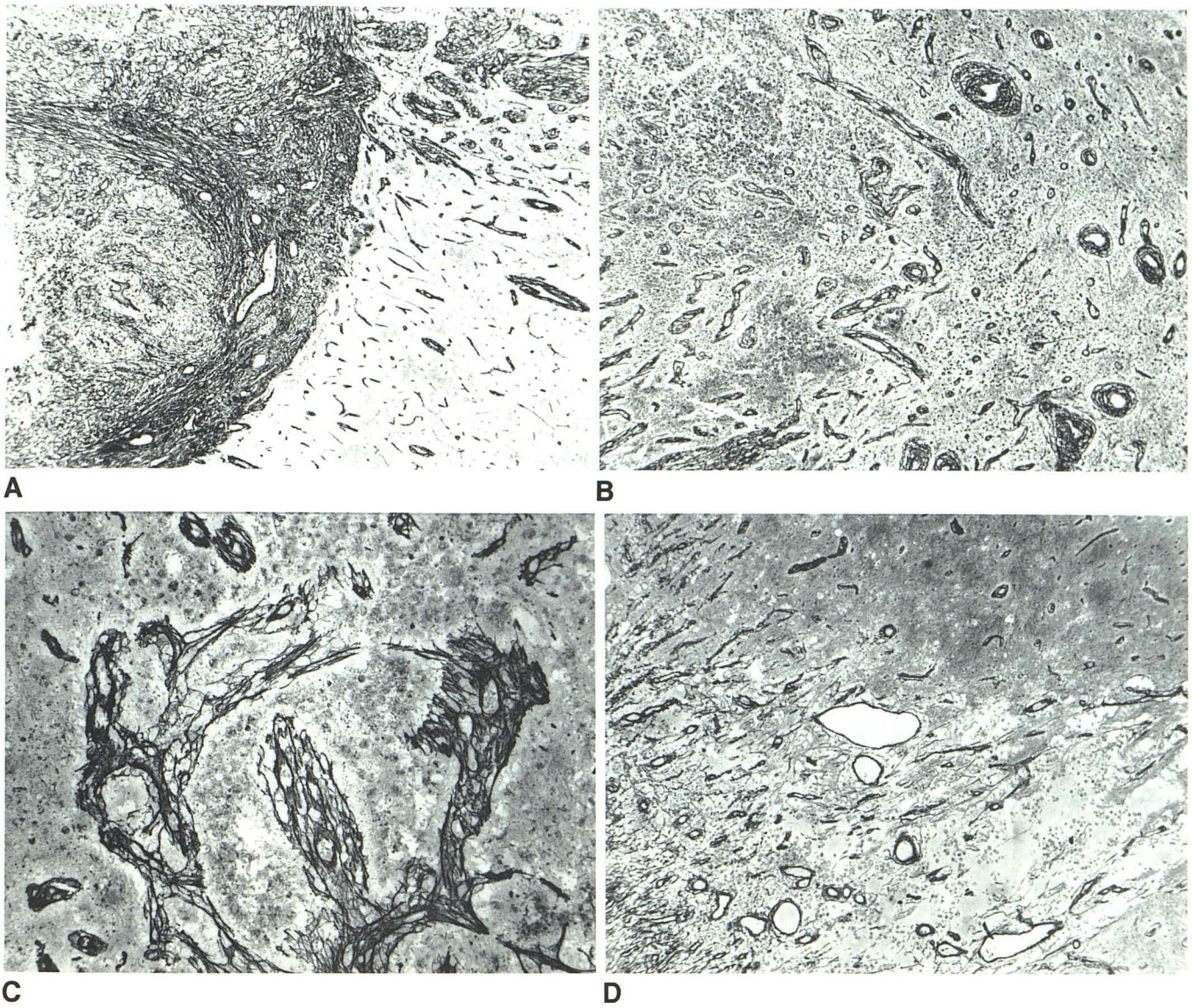

Fig. 6.—Normal capsule formation as depicted by reticulin stain in the late capsule stage (day 21) is contrasted with the phenomenon of fragmentation and "escape." Microscopic views of collagen capsule formation of a 21-day abscess show the difference in development between the cortical and ventricular sides of the abscess. The cortical side showed a dense well-formed network of reticulin and collagen fibers sharply demarcating the edge of the abscess from adjacent parenchyma (**A**). Even at this late stage, however, capsule formation on the ventricular side of the abscess was still incomplete (**B**). Although perivascular reticulin formation was present, these fibers had not yet coalesced to form a complete capsule. The fragmentation of reticulin became evident in the late cerebritis and early capsule stages, as in this day-9 staphylococcal abscess (**C**). Such fragmentation occurred after an attempt at capsule formation failed and the infectious process spread beyond its limits. The vessels around which the reticulin was forming presumably thrombosed and ended up engulfed in the expanding area of necrosis (reticulin ×125). Fragmentation was characterized by rough-edged, irregular, acutely angled clumps of reticulin. **D**, This photomicrograph demonstrates the phenomenon of "escape." The abscess (day 21) already had a well-formed capsule, the periphery of which is seen on the left-hand side of the image. Areas of edema, proteinaceous fluid, and necrosis were evident beyond the confines of the capsules, as seen in the lower-right portion of the image (reticulin, ×50).

were seen on the edge of the necrosis, and within and outside the capsule in perivascular distributions. The amount of surrounding edema had now decreased. Despite these stable findings there were still areas of "escape," where necrosis and collections of protein-rich fluid were identified beyond the confines of the collagenous capsule (see Fig. 6D). The capsule was thick enough, however, so that no significant fragmentation occurred. The difference between the cortical and ventricular sides of the abscess, in terms of capsule development and thickness, was evident at this late stage (see Fig. 6A and B), especially where ventricular rupture had occurred (see Fig. 1B).

The CT scan findings showed a low-density lesion of smaller size and with persistent but smaller-diameter ring-contrast enhancement than in the previous stage (see Fig. 7). Surrounding edema had further decreased. The combination of these phenomena led to a significant decrease in mass effect. If ependymitis was identified at an earlier stage, ventricular contrast enhancement persisted, and ventricular dilation had increased. Time-density curves of contrast enhance-

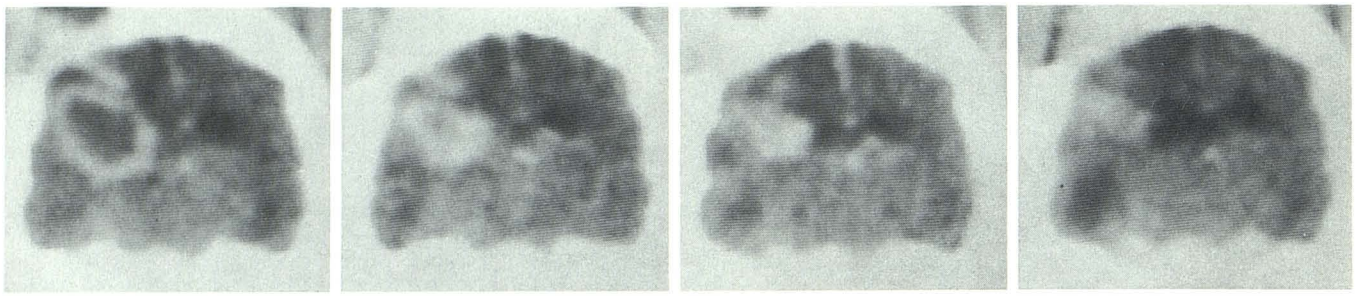

Fig. 7.—Postcontrast CT scans (5 min) of a staphylococcal abscess on days 9 (**A**), 14 (**B**), 18 (**C**), and 21 (**D**) following inoculation. This series shows the contrast-enhancing ring at its maximum size in the late cerebritis stage and its progressive decrease in diameter through the capsule stages. Note the progressive ventricular enlargement as the size of the abscess decreases. The right temporal horn is trapped, since it was visible on day 14 and became progressively larger through day 21.

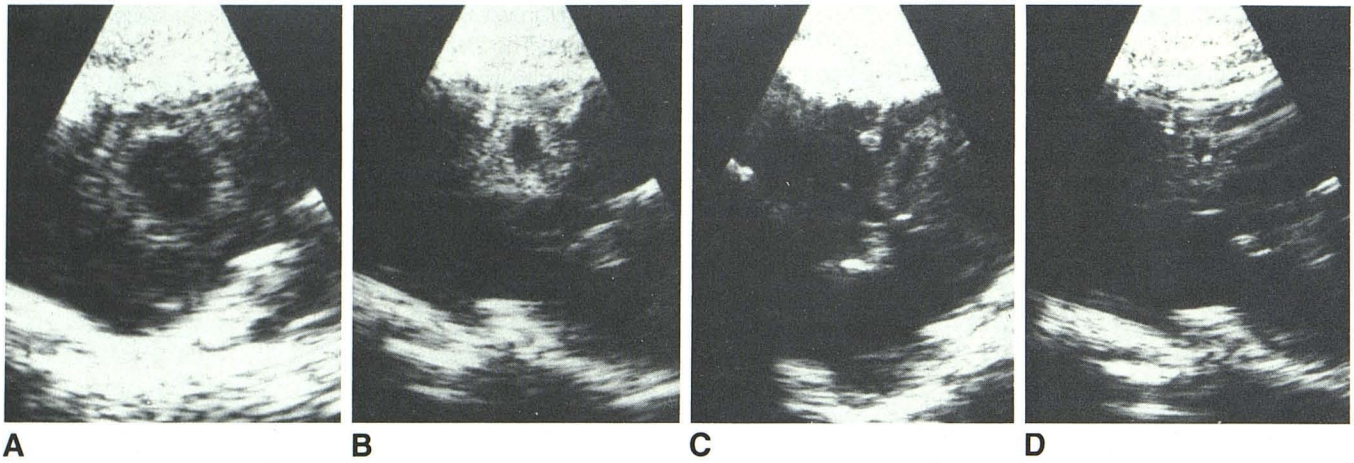

Fig. 8.—Serial sagittal US scans of the same staphylococcal abscess shown in Figure 7: days 9 (**A**), 14 (**B**), 18 (**C**) and 21 (**D**). The abscess was at its maximum size at day 9. As the abscess healed, the diameter of the hyperechoic ring decreased and its thickness increased. Compared with the CT scans, the US scans provide better definition of the small necrotic center seen late in the capsule stage (**D**).

ment did not clearly discriminate the capsule stage from the cerebritis stage, either in terms of magnitude (30 to 40 Hounsfield units above baseline) or pattern of enhancement (other than size). The US scan showed a similar decrease in the hypoechoic center and hyperechoic ring (see Fig. 8). At this stage, the hyperechoic ring correlated with the collagenous capsule.

Ventricular Rupture

Six of the 13 animals demonstrated, histologically and by imaging methods, ventricular rupture of the infection. Histologically, the characteristic finding was rupture of the ependyma with inflammatory cells spilling into the ventricular system and infiltrating the choroid plexus (see Fig. 2). The marked inflammatory infiltrate caused the choroid plexus to increase in size. Ventricular rupture, which could be seen on the CT scan as early as day 3, was evidenced by the low-density lesion abutting the ventricular system and the abnormal, prominent contrast enhancement of the ipsilateral choroid plexus (see Fig. 4). It was not until the early capsule stage that enhancement beyond the choroid plexus was seen within the ventricular system. Ventricular dilation was noted concurrently, a condition that progressed into the late capsule stage while the degree of contrast enhancement within the ventricles remained stable. Trapped ipsilateral temporal horns were common (see Fig. 7). It was possible for the parenchymal contrast-enhancing lesion to decrease in size while ventricular contrast enhancement remained unchanged or increased (Fig. 9).

Discussion

The experimental model of *Staphylococcus aureus* brain abscess showed, both neuropathologically and by imaging tests, a number of similarities to experimental brain abscess caused by other organisms. In general, the neuropathologic stages from the time of inoculation to near resolution are relatively stereotyped for all the bacterial organisms studied. What the staphylococcus model shows, however, is that there

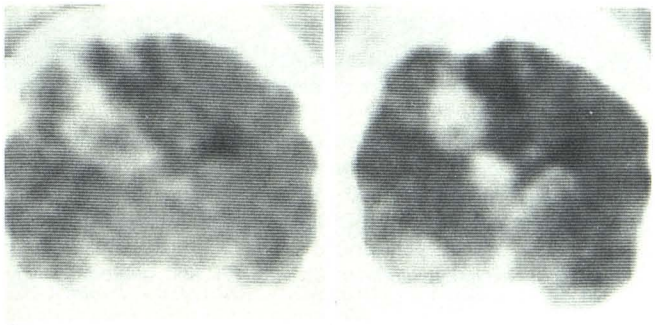

A B

Fig. 9.—Postcontrast CT scans (10 min postinfusion) of an abscess on day 7 (**A**) and day 14 (**B**) after inoculation. Ring enhancement, as well as "pointing" of the abscess toward the ventricular system, were evident in the late cerebritis stage (**A**). In the early capsule stage, ventricular rupture was present with marked enhancement in both lateral ventricles and the right temporal horn (**B**). The parenchymal lesion was smaller than on day 7.

may be significant quantitative differences among the more virulent organisms. Virulence may be related to the numerous enzymes (such as coagulase, staphylokinase, and hyaluronidase) and toxins (several types of hemolysins, leukocidin) produced by this bacteria. The amount of necrosis and the total area of involvement with staphylococcus was greater than the alpha streptococcus, even though the number of bacteria in the inoculum was similar. Compared with the less virulent organism alpha streptococcus, the quantity of necrosis and inflammation was greater with staphylococcus, and the course of the infection as it progressed toward resolution was prolonged. Moreover, it took longer for the infection to reach a stable size than with alpha streptococcus, and it also took longer to wall off the necrotic region with a collagenous capsule. Separation between stages was not as distinct as with alpha streptococcus, so it was not unusual for the abscess, in either the early or late capsule stage, to contain segments that were still in the early or late cerebritis stage, indicating recent extension. Similarly, the time-density curves for the cerebritis and capsule stages did not cleanly distinguish these stages as they did for alpha streptococcus. The thickening of the ring-contrast enhancement, although not as prominent as in alpha streptococcus, did discriminate between the cerebritis and capsule stages. Further evidence of greater and more rapid spread was the high incidence of ependymitis. Ependymitis was apparent, both neuropathologically and by imaging tests, early in the pathogenesis of the abscess.

In addition to the above quantitative differences, some qualitative differences were also noted. Of particular interest was the susceptibility of white matter to destruction by infection while the overlying gray matter remained relatively resistant. In fact, the infectious and inflammatory process could be seen to extend throughout the white matter, causing necrosis under several gyri, while the overlying gray matter was spared of necrosis, exhibiting only minimal cerebritis. The spread of infection did not seem to follow any particular course of white-matter tracts, and the susceptibility of white matter caused the inflammation to spread rapidly to the ventricular system, since it was not far away. As compared with the more benign organism alpha streptococcus, *Staphylococcus aureus* showed both a high incidence and an early appearance of ependymitis.

Another phenomenon that differed qualitatively from the alpha streptococcus brain abscess was that of "escape" of inflammation beyond the developing capsule. In both the early and late capsule stages there was histologic evidence for extension of inflammation, necrosis, and edema beyond what appeared to be a relatively well formed capsule. These "escape" points were indicative of the virulence of the organism and were also seen with *B. fragilis* [10].

In general, the CT and ultrasound scans reflected the pathologic changes accurately. The size of the lesions, as evidenced by their density and their progression on CT, accurately defined the tempo of the pathologic changes. The low-density central regions represented necrosis, and they did not fill in with contrast on delayed scans, since they were avascular. The lack of filling-in differed from alpha streptococcus and reflected the more rapid development of inflammatory necrosis, which is avascular and does not exhibit contrast enhancement. The degree of contrast enhancement correlated with the presence and severity of the inflammatory infiltrate. In areas where no enhancement was detected, pathologic findings confirmed a near lack of inflammatory infiltrate. This latter finding often represented sites of rapid extension of the infection. The CT scan could, therefore, be insensitive to the most aggressive portions of the lesion. The time-density curves of the ring-contrast enhancement were not as reliable in the staphylococcus brain abscess model as they were in alpha streptococcus in terms of their ability to differentiate the cerebritis from the capsule stage. This is because of the delay in capsule formation and the phenomenon of "escape," which caused the capsule stage to consist of a collagenous capsule with areas of cerebritis. This heterogeneity obscured measurable differences in contrast enhancement between these stages.

The US scan accurately depicted the size of the lesion, showing necrosis to be hypoechoic. The echogenic ring correlated with the inflammatory region around the necrosis. Both the US and CT scans showed the lesion to be at its maximum size in the cerebritis stage, and both scans showed that the diameter of the ring lesion, as seen on CT or US, decreased as capsule formation took place and as the necrotic center decreased. With this decrease in size, the hyperechoic ring thickened and the collagen capsule developed. Owing to the increased contrast enhancement of the choroid plexus, the CT scan was more sensitive than the US scan in detecting the early development of ependymitis. The US scan detected increased echogenicity of the choroid plexus, but differentiation from the normal choroid plexus was not as certain as with CT. Not until approximately 14 days after inoculation could additional abnormal contrast enhancement within the ventricles be defined beyond the choroid plexus. Ventricular enlargement always accompanied other evidence for ependymitis. Asymmetric ventricular enlargement occurred in the late cerebritis stage; trapped temporal horns contributed to this asymmetry.

The findings in this experimental staphylococcus brain abscess model call into question the spread of bacterial infection within the brain and the role of capsule formation. The findings in this staphylococcus brain abscess model suggest that white matter is much more susceptible than gray matter to bacterial invasion and destruction. Both the *Staphylococcus aureus* and *Bacteroides fragilis* organisms caused extensive necrosis in white matter while distinctly sparing overlying gray matter. The gray matter never showed necrosis, despite extensive and immediately adjacent necrosis of white matter under several gyri. Gray-matter involvement was limited to perivascular acute inflammatory infiltrates. Since the site of inoculation was deep in the parietal white matter, the infection's rapid spread to the ventricular system was not unexpected. Moreover, the path to the ventricular system seemed to offer the least resistance, a phenomenon that may be related to the size of the extracellular space. The manner of spread to the ventricular system appeared to be centrifugal and did not appear to follow any particular white-matter tracks. The spread of infection described in an *E. coli* brain abscess model may also reflect the susceptibility of white matter to infection rather than the tendency of infection to spread along specific white-matter tracts [18]. This susceptibility of white matter to bacterial infection is especially prominent in early brain development as evidenced by gram-negative meningoencephalitis seen in neonates. We have seen extensive destruction of neonatal hemispheric white matter by such diverse but virulent organisms as *Aspergillus* and *Citrobacter*. The reason for the relative sparing of gray matter in these bacterial infections is not clear.

The size of the bacterial abscess reached a maximum in the late cerebritis stage before any significant capsule formation had taken place. The host was therefore able to contain the infectious process, and the gray matter was spared long before significant capsule formation occurred. Capsule formation seemed to be more a mechanism for introducing fibroblasts and macrophages to the area of tissue destruction for the clean-up phase of healing than it was a means for containing the infection. The quantitative difference between the cortical and ventricular sides in reticulin and collagen production was accentuated in the staphylococcal model. This cortical–ventricular difference, however, rather than being an active factor in directing the infectious spread, appeared to be a more passive phenomenon. Spread to the ventricle often occurred before significant reticulin or collagen was detected. Greater collagen production occurred in well-vascularized tissue that was essentially intact. Since white matter was rapidly destroyed, the developing capsule had difficulty finding a foothold. Even when capsule development began in the form of perivascular reticulin formation, the virulent organism staphylococcus caused an expanding necrosis, which simply left initial capsule development in its wake. Destruction and fragmentation of reticulin was commonly seen with staphylococcus in both the late cerebritis and early capsule stages. Even in the late capsule stage, with generous capsule formation, areas of "escape" of inflammation extended outside the capsule. All these findings call into question the "containment" role of capsule formation.

REFERENCES

1. Enzmann DR, Britt RH, Yeager AS. Experimental brain abscess evolution, computed tomographic and neuropathologic correlation. *Radiology* **1979**;133:113–122
2. Britt RH, Enzmann DR, Yeager AS. Neuropathologic and computerized tomographic findings in experimental brain abscess. *Neurosurgery* **1981**;55:590–603
3. Enzmann DR, Britt RH, Lyons B, Carroll B, Wilson DA, Buxton JA. High resolution ultrasound evaluation of experimental brain abscess evolution: comparison with CT and neuropathology. *Radiology* **1982**;142:95–102
4. Enzmann DR, Lyons BE, Carroll B, et al. Experimental brain abscess: enhanced sonography and pathologic correlation. *AJNR* **1982**;3:41–45
5. Lyons B, Enzmann DR, Britt RH, Obana W, Placone RC, Yeager AS. Short-term, high-dose corticosteroids in computed tomographic staging of experimental brain abscess. *Neuroradiology* **1982**;23:279–284
6. Enzmann DR, Britt RH, Placone RC, Obana W, Lyons B, Yeager AS. The effect of short-term corticosteroids on the CT appearance of experimental brain abscess. *Radiology* **1982**;145:79–84
7. Enzmann DR, Britt RH, Placone R. Staging of human brain abscess by computed tomography. *Radiology* **1983**;146:703–708
8. Brant-Zawadzki M, Enzmann DR, Placone RC Jr, et al. NMR imaging of experimental brain abscess: comparison with CT. *AJNR* **1983**;4:250–253
9. Britt RH, Enzmann DR. Clinical stages of human brain abscesses on serial CT scans after contrast infusion: computerized tomography, neuropathological and clinical correlations. *J Neurosurg* **1983**;59:972–989
10. Britt RH, Enzmann DR, Placone RC, Obana WG, Yeager AS. Experimental anaerobic brain abscess. *J Neurosurg* **1984**; 60:1148–1159
11. Enzmann DR, Placone RC, Britt RH. Dynamic computed tomographic scans in experimental brain abscess. *Neuroradiology* **1984**;26:309–313
12. Wood JH, Lightfoote WE II, Ommaya AK. Cerebral abscesses produced by bacterial implantation and septic embolisation in primates. *J Neurol Neurosurg Psychiatry* **1979**;42:63–69
13. Winn HR, Mendes M, Moore P, Wheeler C, Rodeheaver G. Production of experimental brain abscess in the rat. *J Neurosurg* **1979**;51:685–690
14. Falconer MA, McFarlan AM, Russell DS. Experimental brain abscesses in the rabbit. *Br J Surg* **1943**;30:245–260
15. Hassler O, Forsgren A. Experimental abscesses in brain and subcutis: a microangiographic study in the rabbit. *Acta Pathol Microbiol Immunol Scand* **1964**;62:59–67
16. Quartey GRC, Johnston JA, Rozdilsky B. Decadron in the treatment of cerebral abscess. *Neurosurgery* **1976**;45:301–310
17. Molinari GF, Smith L, Goldstein MN, Satran R. Brain abscess from septic cerebral embolism: an experimental model. *Neurology* **1973**;23:1205–1210
18. Neuwelt EA, Lawrence MS, Blank NK. Effect of gentamicin and dexamethasone on the natural history of the rat *Escherichia coli* brain abscess model with histopathological correlation. *Neurosurgery* **1984**;15:475–483
19. Onderdonk AB, Kasper DL, Masheim BJ, Louie TJ, Gorbach SL, Bartlett JG. Experimental animal models for anaerobic infections. *Rev Infect Dis* **1979**;1:291–301
20. Kretzschmar K, Wallenfang T, Bohl J. CT studies of brain abscesses in cats. *Neuroradiology* **1981**;22:93–98
21. Wallenfang T, Bohl J, Kretzschmar K. Evolution of brain abscess in cats: formation of capsule and resolution of brain edema. *Neurosurg Rev* **1980**;3:101–111